JOURNAL OF SOLID STATE CHEMISTRY 115, 158–164 (1995)

Synthesis and Crystal Structure of Orthorhombic $NaSn_2Cl_5$: A New Type of AB_2X_5 Compound

Zhibin Zhang and Heinz Dieter Lutz[1]

Universität-GH-Siegen, Anorganische Chemie I, D-57068 Siegen, Germany

Received May 5, 1994; accepted August 18, 1994

DEDICATED TO PROFESSOR HANS UWE SCHUSTER† ON THE OCCASION OF HIS 65TH BIRTHDAY

The phase diagram of the quasi-binary system $NaCl–SnCl_2$ has been derived from DSC and X-ray investigations. In this system a dystectic $NaSn_2Cl_5$ compound phase was found, which was obtained by grinding mixtures of NaCl and $SnCl_2$ in a closed ball mill and then subsequent tempering at temperatures about 170°C in evacuated sealed silica ampoules. The single-crystal structure of $NaSn_2Cl_5$ was determined. It crystallizes with a new orthorhombic-type arrangement [space group *Pnnm*; a = 818.09(5), b = 1203.1(1), c = 871.63(8) pm; Z = 4]. The structure was solved by Patterson methods with the MolEN program, and refined to a final R value of 0.019 for 717 unique reflections. The sodium ions are located in almost octahedral voids of Cl ions. Two kinds of tin ions manifest themselves structurally by a great distortion of their coordination environment, three Cl ions are situated at <272.77 pm from the tin ion, which is a reasonable Sn–Cl bond length, but the other five or six are repelled by the lone pair to distances of >306.75 pm. Different from the structure of U_3Se_5, it is another distorted Rh_5Ge_3 structure. In this paper the structural relationship between $NH_4Pb_2Cl_5$ and $NaSn_2Cl_5$ is elucidated systematically by means of the group theoretical representation of group–subgroup relations.

INTRODUCTION

Ternary halides of the formula AB_2X_5 (A = K, In, Tl, NH_4; B = Sr, Sn, Pb; X = Cl, Br, I) have been the object of investigation for a long time, and early work dates back to the beginning of this century. They were often prepared from aqueous solutions containing the binary compounds in appropriate concentrations. In the course of thermoanalytical studies of quasi-binary systems $AX–BX_2$, many of these compounds were discovered as dystectic or peritectic points in the phase diagrams, but there were contradictory findings abounding in the literature.

In 1937, Powell and Tasker (1) reported on the structure of $NH_4Pb_2Br_5$, they had prepared from aqueous solution. Later an orthorhombic polymorph was described, and in 1968 Jansen (2) discovered a whole series of such "orthorhombic" compounds. This investigator, however, prepared these compounds by solid-state reactions. It was not until 1976 that Keller (3) and independently Ras *et al.* (4) elucidated the structure of one of the hitherto "orthorhombic" representatives, viz., that of $NH_4Pb_2Cl_5$, showing that it was monoclinic with almost orthogonal metrics.

In the 1980s, Beck *et al.* (5–7) studied systematically several series of AB_2X_5 compounds containing ns^2 cations with an inert or lone electron pair in the A or B position, in both or in one of them. They pointed out that all known AB_2X_5 compounds of this family can clearly be separated into the monoclinic $NH_4Pb_2Cl_5$ type and the tetragonal $NH_4Pb_2Br_5$ type on the basis of the size relations A/X and B/X. The former is stabilized by lower A/X and higher B/X values, the latter is stabilized by larger A and smaller B ions.

The NaCl–$SnCl_2$ system has not been described until now, although in 1913 Rack (8) and in 1988 Beck and Nau (9) reported on it. Due to synthetic difficulties, a ternary compound was not found. In this paper, one way to yield such a compound in a more convenient way is introduced. Orthorhombic $NaSn_2Cl_5$, a very distorted Rh_5Ge_3-type new structure, is reported for the first time.

EXPERIMENTAL

1. Preparation of the Starting Materials

In order to avoid the formation of hydrates and other by-products, all starting materials and the products were synthesized and handled under dry argon gas. The NaCl used (Merck p.a. grade) was dried under vacuum at temperatures up to 300°C for about 3 hr. The preparation of anhydrous stannous chloride (10) was achieved by treatment of the hydrate $SnCl_2 \cdot 2H_2O$ with acetic anhydride. The dehydration was almost instantaneous, much heat was evolved. The anhydrous salt separated, and after being washed free from acetic acid with dry ether it was dried at temperature 110°C for several hours.

[1] To whom correspondence should be addressed.

† Professor Schuster died in November 1994.

0022-4596/95 $6.00

2. Polycrystalline Samples

Polycrystalline samples of ternary halides in the NaCl–$SnCl_2$ system were synthesized by grinding appropriate mixtures of NaCl and $SnCl_2$ in closed ball mills for several hours, subsequently pressing them together under about 5 tons, and then annealing for 4 weeks at temperatures about 170°C in evacuated sealed quartz ampoules.

All starting materials and products were characterized by X-ray analysis using the Guinier-600 camera technique with Quartz as internal standard (α-SiO_2, a = 491.36 pm and c = 540.54 pm), using Cu$K\alpha_1$ radiation. The unit-cell dimensions of $NaSn_2Cl_5$ were calculated by means of least-squares methods (LSUCR) (11). High-temperature X-ray diffraction patterns were obtained with an Enraf–Nonius Guinier Simon FR533 camera, using Cu$K\alpha_1$ radiation. The samples were sealed in quartz capillaries taken for sample holders. The heating and cooling rates used were 10°C/hr and the running rate of the film was 1.5 mm/hr. The experimental density was measured pyknometrically under an argon gas box.

Differential scanning calorimetry (DSC) measurements were performed with a Perkin–Elmer DSC7 calorimeter, with samples (~5 mg) sealed in closed gold crucibles. An empty sample pan was used as a reference. The heating rates were 5 ~ 10°C/min. For temperature calibration, the melting points and phase transitions of KNO_3 and AgCl were used.

Raman spectra, with samples taken in sealed glass capillary tubes, were measured on a Dilor OMARS 89 multichannel Raman spectrograph with the usual right-angle geometry (spectral slit width <4 cm^{-1}). For excitation, the 514.5-nm line of an Ar^+ ion laser was employed (laser power at the sample was about 150 mW). The integration time was 1–30 sec; the number of accumulations were 30–50. Infrared spectra were recorded on a Bruker IFS 113 v Fourier transform interferometer (resolution <4 cm^{-1}), using Nuyol mull as matrices.

3. Single Crystals

Colorless crystals of $NaSn_2Cl_5$ were grown by fusing a stoichiometric mixture of NaCl and $SnCl_2$ and tempering at temperatures about 165°C for about several weeks.

A crystal with well developed faces of the approximate size 0.12 × 0.2 × 0.25 mm was mounted in a sealed glass capillary. The space group was inferred from precession photographs of $hk0$, $hk1$, $hk2$, $h0l$, $h1l$, and $h2l$ layers with a Buerger precession camera (Firma Huber, Rimsting). Intensity data were collected to $2\theta < 49.8°$ on an Enraf–Nonius CAD4 diffractometer using graphite-monochromatized Mo$K\alpha$ radiation (λ = 0.71069 Å) (12). An orientation matrix for data collection were obtained from least-squares refinements, using the setting angles of 25 reflections in the range $16° < \theta < 24°$, measured by the computer controlled diagonal slit method of centering. The intensities of three standard reflections were checked every 166 min, and orientation control was performed every 200 measured reflections. The data were corrected for Lorentz and polarization effects. Empirical absorption corrections from the program Enraf–Nonius were applied to the data. The structure of $NaSn_2Cl_5$ was solved by using the program MolEN (13).

RESULTS AND DISCUSSION

1. The NaCl–$SnCl_2$ System

On the basis of the data obtained from DSC and X-ray phase analyses the equilibrium diagram of the NaCl–$SnCl_2$ system is given in Fig. 1. Tin(II) chloride forms one compound with sodium chloride $NaSn_2Cl_5$. The compound melts congruently at 205°C, and there are no polymorphic transformations up to the melting point.

2. Synthesis of Monophase Samples of $NaSn_2Cl_5$

Because there are large differences in the melting points between NaCl (800°C) and $SnCl_2$ (240°C) and the reactivity of the products formed is quite slow, mixtures of the reactants and products always were obtained by normal ceramic or fusing methods. In order to speed up reaction rates, in the solid-state system, normally it is recommended to raise the temperature as high as possible. In this system, however, additional problems occur at high temperatures, e.g., the volatilization of $SnCl_2$. So

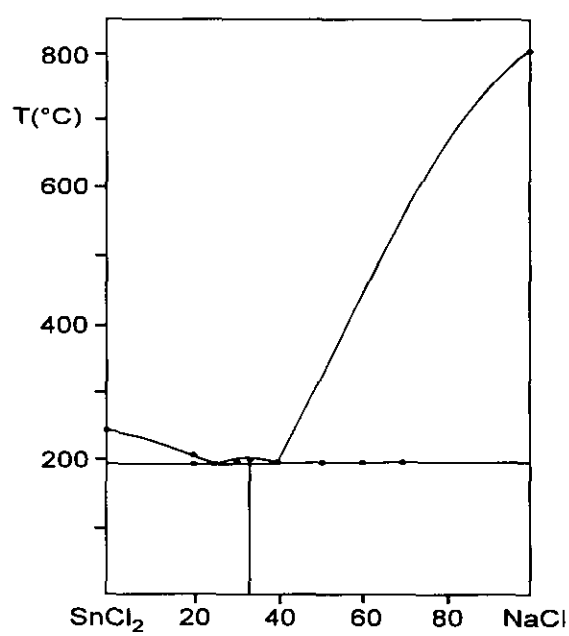

FIG. 1. Phase diagram of the NaCl–$SnCl_2$ system.

the reaction takes place only at ~170°C, relatively, a low temperature. On the basis of this view, we have synthesized single-phase $NaSn_2Cl_5$ by means of grinding mill and long-time tempering techniques.

3. Crystal Structure

Precession photographs of $NaSn_2Cl_5$ display mmm symmetry with extinctions ($0kl$, with $k + l = 2n$, $h0l$ with $h + l = 2n$, and $h00$, $0k0$, and $00l$ with $h = 2n$, $k = 2n$, and $l = 2n$ respectively), which are characteristic of space groups *Pnnm* and *Pnn*2. The centrosymmetric group was found to be correct during the structure refinement.

The structure was solved using the Patterson heavy-atom method, which revealed the positions of two atoms. The remaining atoms were located in succeeding difference Fourier syntheses. The structure was refined with a full-matrix least-squares treatment, where the function minimized was $w(|F_o| - |F_c|)^2$ and the weight w is defined at $1/\sigma^2(F)$ for all observed reflections. Anomalous dispersion effects were included in F_c, the values for f' and f'' were taken from Cromer and Waber (14). Only the 649 reflections with $[|F_o| \geq 2.0\sigma(F_o)]$ were used in the refinements. The final cycle of refinement included 45 variable parameters and converged (largest parameter shift was 0.01 times is esd) to R and R_w is 0.019 and 0.026, respectively. The final difference Fourier map showed no significant residual electron density. The results of the refinement procedures are given in Tables 1, 2, and 3. Table 4 contains a list of all interatomic distances and angles.

TABLE 1
Crystal Data, Data-Collection Parameters, and Details of Structure Refinements for $NaSn_2Cl_5$

Space group	*Pnnm* (No. 58)
Lattice constants[a] (pm)	a = 818.09(5)
	b = 1203.1(1)
	c = 871.63(8)
Unit cell volume (pm^3)	$V = 857.93(9) \times 10^6$
	Z = 4
Calculated density (g cm^{-3})	d_{th} = 3.39
Crystal dimensions (mm)	0.12 × 0.2 × 0.25
Temperature measured	293 K
Scan mode	$\omega/2\theta$-scan
Measured region $2\theta_{max}$	49.8°
h, k, l ranges	$0 \leq h \leq 9$, $-14 \leq k \leq 14$, $0 \leq l \leq 10$
No. of reflections measured	1389
No. of observed reflections $F_o > 2.0\sigma F_o$	649
No. of unique reflections	717
Parameters refined	45
Linear absorption coefficient	$\mu_{MoK\alpha}$ = 73.82 cm^{-1}
Extinction coefficient	$1.23(1) \times 10^{-6}$
Unweighted agreement factor	R = 0.019
Weighted agreement factor	R_w = 0.026
Weighting scheme	$w = 1/\sigma^2(F)$
	s = 1.951
$\Delta\rho_{max}$ (e pm^{-3})	0.670×10^{-6}
$\Delta\rho_{min}$ (e pm^{-3})	-0.830×10^{-6}
Computer software	MolEN (Enraf–Nonius)

[a] Obtained from Guinier photograph.

TABLE 2
Fractional Atomic Coordinates and Isotropic Thermal Parameters of $NaSn_2Cl_5$

Atom	Site	x	y	z	B_{iso}
Na	4*f*	0.0	0.5	0.2527(1)	2.85(4)
Sn(1)	4*g*	0.04135(3)	0.16892(2)	0.0	2.014(5)
Sn(2)	4*g*	0.54279(3)	0.32717(2)	0.0	1.948(5)
Cl(1)	8*h*	0.17276(8)	0.29129(6)	0.28304(7)	2.31(1)
Cl(2)	4*g*	0.1885(1)	0.56338(9)	0.0	2.73(2)
Cl(3)	4*g*	0.33654(9)	0.10193(8)	0.0	2.05(1)
Cl(4)	4*e*	0.0	0.0	0.2051(1)	2.23(2)

Note. $B_{eq} = 4/3 \sum_i \sum_j \beta_{ij} a_i^* a_j^*$.

In the $NaSn_2Cl_5$-type structure, the Sn ions are found in strongly distorted trigonal prisms of Cl ions with three additional Cl ions capping this polyhedron. The tricapped trigonal prisms are joined along [001] by common triangular faces, containing two kinds of tin ions alternatively. Two such polyhedra share the edge; these double prisms are connected by sharing the "free" edges of other double prisms given a pseudohexagonal arrangement, such structural units are again interconnected within the (001) planes in same manner, which is shown in Fig. 2. Three Cl ions on one side of the tin are at ≤272.77 pm, which is a reasonable Sn–Cl bond length, but the other are repelled by the lone pair to distances of >306.75 pm. The Na^+ ions lie along pseudohexagonal axes with different z parameters. Sodium is coordianted to six Cl atoms forming a slightly distorted octahedron with Na–Cl distances varying between 279.48(9) and 289.35(7) pm (Fig. 3). The distortion of the $NaCl_6$ octahedra results from sharing edges between them and corners with trigonal $SnCl_6$ prisms.

TABLE 3
Anisotropic Thermal Parameters (U_{ij}/100 pm^2) of $NaSn_2Cl_5$

Atom	U_{11}	U_{22}	U_{33}	U_{12}	U_{13}	U_{23}
Na	5.3(1)	2.8(1)	2.66(9)	−0.2(1)	0.0	0.0
Sn(1)	2.17(1)	2.29(1)	2.19(1)	0.19(1)	0.0	0.0
Sn(2)	2.32(1)	2.61(1)	2.47(1)	0.05(1)	0.0	0.0
Cl(1)	3.36(3)	2.72(4)	2.70(2)	0.12(3)	0.62(3)	0.31(3)
Cl(2)	3.36(4)	4.32(5)	2.68(4)	−0.162(4)	0.0	0.0
Cl(3)	1.91(3)	3.11(4)	2.79(4)	0.14(4)	0.0	0.0
Cl(4)	3.90(4)	2.63(5)	1.94(3)	−0.45(4)	0.0	0.0

Note. U_{ij} is defined as $T = \exp(-2\pi^2 \sum_i \sum_j U_{ij} h_i h_j a_i^* a_j^*)$.

TABLE 4
Interatomic Distances (pm) and Angles (°) of $NaSn_2Cl_5$

Na^0–$Cl(1)^{0,1}$	289.35(7)	$Cl(1)^0$–Na^0–$Cl(1)^1$	169.51(4)
Na^0–$Cl(2)^{0,2}$	279.48(9)	$Cl(1)^{0,1}$–Na^0–$Cl(2)^{0,2}$	92.25(3)
Na^0–$Cl(3)^{3,4}$	281.75(9)	$Cl(1)^{0,1}$–Na^0–$Cl(2)^{2,0}$	96.01(3)
		$Cl(1)^{0,1}$–Na^0–$Cl(3)^{3,4}$	94.36(3)
$Sn(1)^0$–$Cl(3)^0$	254.59(8)	$Cl(1)^{0,1}$–Na^0–$Cl(3)^{4,3}$	77.54(3)
$Sn(1)^0$–$Cl(4)^{0,8}$	272.77(6)	$Cl(2)^0$–Na^0–$Cl(2)^2$	75.98(3)
$Sn(1)^0$–$Cl(1)^{0,5}$	306.75(7)	$Cl(2)^{0,2}$–Na^0–$Cl(3)^{3,4}$	102.85(2)
$Sn(1)^0$–$Cl(1)^{6,7}$	359.14(7)	$Cl(2)^{0,2}$–Na^0–$Cl(3)^{4,3}$	169.60(3)
$Sn(1)^0$–$Cl(2)^2$	372.9(1)	$Cl(3)^3$–Na^0–$Cl(3)^4$	80.18(3)
$Sn(2)^0$–$Cl(2)^9$	256.25(9)	$Cl(1)^0$–$Sn(1)^0$–$Cl(1)^5$	107.08(2)
$Sn(2)^0$–$Cl(1)^{10,11}$	259.58(7)	$Cl(1)^{0,5}$–$Sn(1)^0$–$Cl(3)^{0,0}$	79.60(2)
$Sn(2)^0$–$Cl(3)^0$	319.2(1)	$Cl(1)^{0,5}$–$Sn(1)^0$–$Cl(4)^{0,8}$	82.76(2)
$Sn(2)^0$–$Cl(4)^{12,10}$	332.46(7)	$Cl(1)^{0,5}$–$Sn(1)^0$–$Cl(4)^{8,0}$	158.15(2)
$Sn(2)^0$–$Cl(1)^{0,5}$	392.89(7)	$Cl(3)^{0,0}$–$Sn(1)^0$–$Cl(4)^{0,8}$	83.21(2)
$Sn(2)^0$–$Cl(2)^0$	405.9(1)	$Cl(4)^0$–$Sn(1)^0$–$Cl(4)^0$	81.90(2)
		$Cl(1)^{10}$–$Sn(2)^0$–$Cl(1)^{11}$	93.53(2)
		$Cl(1)^{10,11}$–$Sn(2)^0$–$Cl(2)^{9,9}$	86.03(2)
		$Cl(1)^{10,11}$–$Sn(2)^0$–$Cl(3)^{0,0}$	75.55(2)
		$Cl(1)^{10,11}$–$Sn(2)^0$–$Cl(4)^{12,10}$	161.77(2)
		$Cl(1)^{10,11}$–$Sn(2)^0$–$Cl(4)^{10,12}$	79.82(2)
		$Cl(2)^0$–$Sn(2)^0$–$Cl(3)^0$	152.83(3)
		$Cl(2)^{9,9}$–$Sn(2)^0$–$Cl(4)^{10,12}$	76.64(2)
		$Cl(3)^0$–$Sn(2)^0$–$Cl(4)^{10,12}$	118.38(1)
		$Cl(4)^{13}$–$Sn(2)^0$–$Cl(4)^{12}$	101.28(2)

Note. (0) x, y, z; (1) $-x, 1-y, z$; (2) $-x, 1-y, -z$; (3) $\frac{1}{2}-x, \frac{1}{2}+y, \frac{1}{2}+z$; (4) $-\frac{1}{2}+x, \frac{1}{2}-y, \frac{1}{2}-z$; (5) $x, y, -z$; (6) $-\frac{1}{2}+x, \frac{1}{2}-y, \frac{1}{2}+z$; (7) $-\frac{1}{2}+x, \frac{1}{2}-y, -\frac{1}{2}+z$; (8) $-x, -y, -z$; (9) $1-x, 1-y, -z$; (10) $\frac{1}{2}+x, \frac{1}{2}-y, \frac{1}{2}-z$; (11) $\frac{1}{2}+x; \frac{1}{2}-y, -\frac{1}{2}+z$; (12) $\frac{1}{2}-x, \frac{1}{2}+y, -\frac{1}{2}+z$.

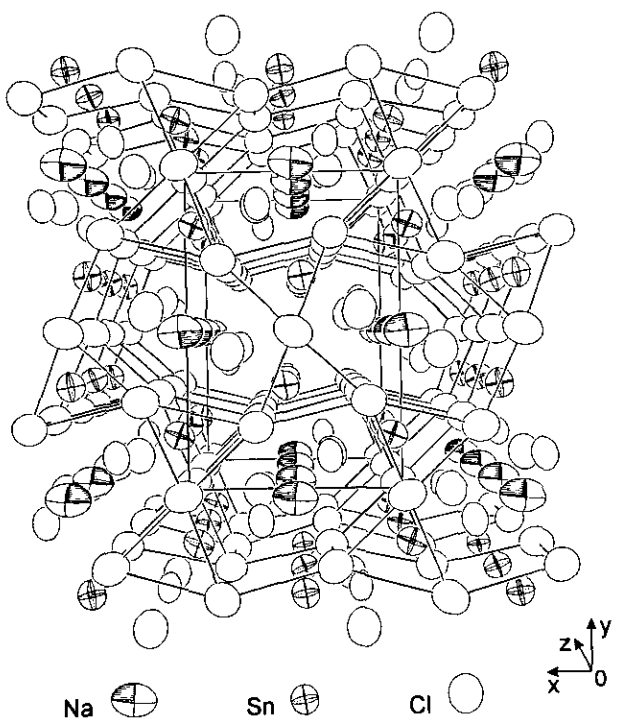

FIG. 2. Crystal structure of orthorhombic $NaSn_2Cl_5$ (Ortep plot, 97% probability).

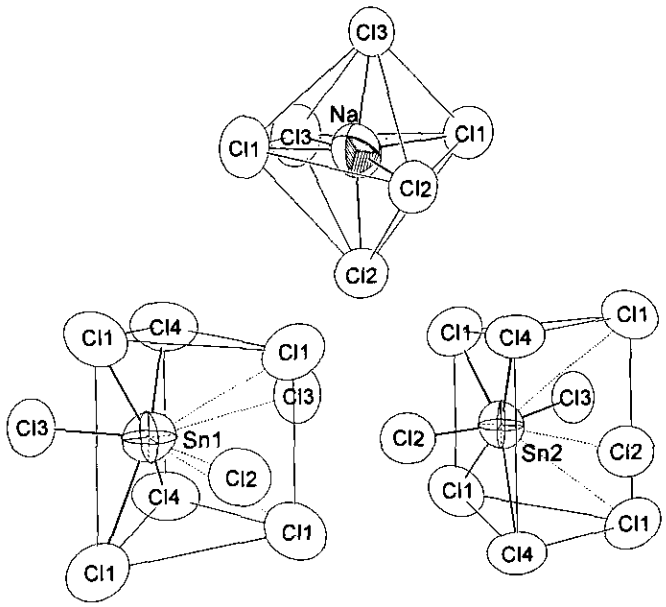

FIG. 3. Slightly distorted $NaCl_6$ octahedron (top) and strongly distorted $SnCl_9$ polyhedra (bottom) in the $NaSn_2Cl_5$ structure.

4. *Raman and IR Spectra of $NaSn_2Cl_5$*

Unit-cell group analysis (D_{2h}^{12}) (15) yields the following distribution of the 96 vibrational modes:

$$\Gamma_{\text{Raman}} = 13A_g + 13B_{1g} + 11B_{2g} + 11B_{3g}$$
$$\Gamma_{\text{infrared}} = 8B_{1u} + 14B_{2u} + 14B_{3u}$$
$$\Gamma_{\text{acoustic}} = B_{1u} + B_{2u} + B_{3u}$$
$$\Gamma_{\text{silent}} = 9A_u.$$

All the Raman bands are located in the 10–300 cm^{-1} spectral region. The 108-K spectrum contains nine bands, viz., at 32, 57, 80, 88, 130, 143, 184, 251, and 265 cm^{-1}. On cooling the samples, the spectrum became better resolved as the line widths narrowed (Fig. 4). The 79 cm^{-1} band is split into two distinct components. In general, the peaks were found to shift to higher frequency on cooling, a behaviour consistent with the expected increase in force constant as the crystal contracted. For instance at 108 K, the 126 and 139 lines shift to 130 and 143 cm^{-1}.

The IR spectra of $NaSn_2Cl_5$ reveal up to eight bands, viz., at 48, 75, 122, 140, 153, 203, 246, and 303 cm^{-1} (see Fig. 5).

5. *Structural Relationships*

So far all AB_2X_5 compounds (A = Na, K, In, Tl, NH_4; B = Sr, Sn, Pb; X = Cl, Br, I) were found to belong to one of three structure types, viz., the $NH_4Pb_2Br_5$ type, space group $I4/mcm$; the $NH_4Pb_2Cl_5$ type, space group $P2_1/c$; and the $NaSn_2Cl_5$ type, space group $Pnnm$. There

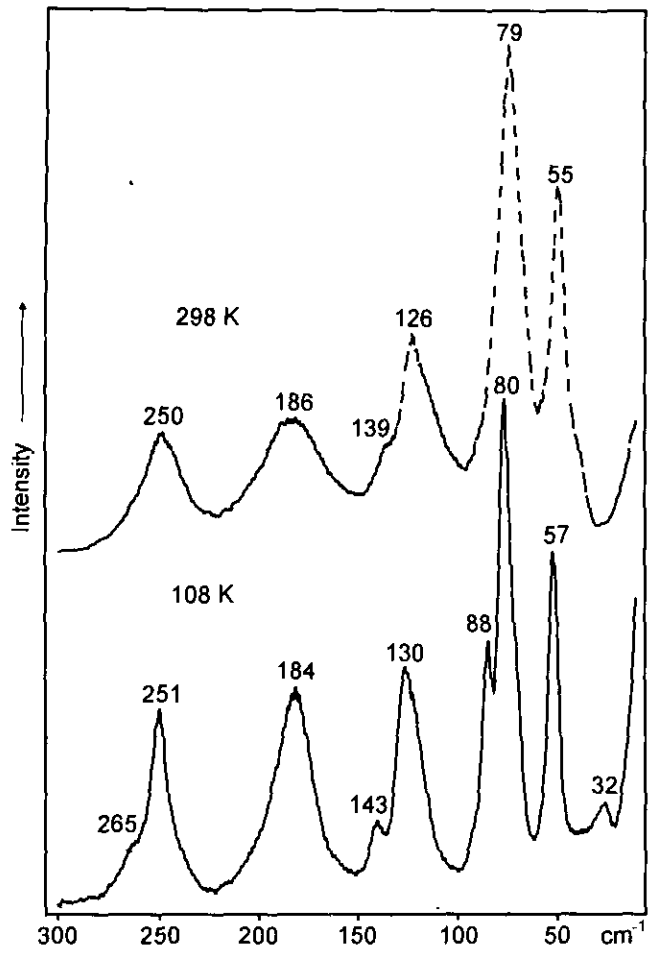

FIG. 4. Raman spectra of $NaSn_2Cl_5$ recorded at ambient temperature (dashed line) and at liquid-nitrogen temperature (full line).

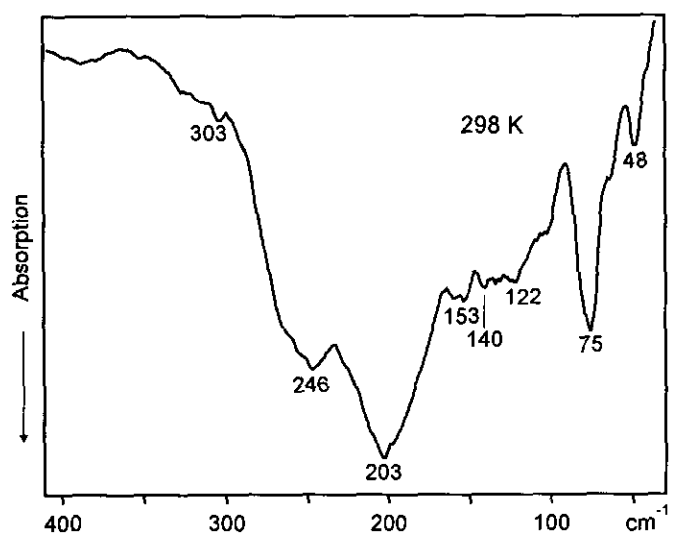

FIG. 5. IR spectrum of $NaSn_2Cl_5$ at ambient temperature.

are close structural relationships between the $NH_4Pb_2Cl_5$ and $NaSn_2Cl_5$ types.

The following family tree (see Fig. 6) is an extension of such a diagram given earlier (16). Chemical formulas in parentheses indicate the content of the unit cell. Vacant sites are indicated by squares. Unconventional settings are used to demonstrate the symmetry relationships more clearly. The Rh_5Ge_3 structure type plays a central role in this family of structures, where the different crystallographic sites of Ge are differentiated chemically. La_2SnS_5 is another example for this structural arrangement.

The U_3Se_5-type structure derives from the Rh_5Ge_3-(anti-)type structure via small distortions, which results in doubling the c axis of U_3Se_5 (or Y_2HfS_5). No interchange of atomic positions is needed to go from one structural type to another (17, 18). In this branch, the $NH_4Pb_2Cl_5$ structure finally results from an additional *translationengleich* reduction with loss of orthogonality, by which different cations are allowed on a formerly equivalent site. The $NaSn_2Cl_5$-type structure is another very distorted version of the Rh_5Ge_3 structure by doubling the *c* axis *klassengleich*, as for U_3Se_5, but where different cations occupy a respective equivalent site.

The Rh_5Ge_3-type structure may be considered as a distorted deficient Fe_2P (=Fe_6P_3)-type structure, where $\frac{1}{6}$ of the Fe positions are unoccupied (19). The U_3Se_5 and

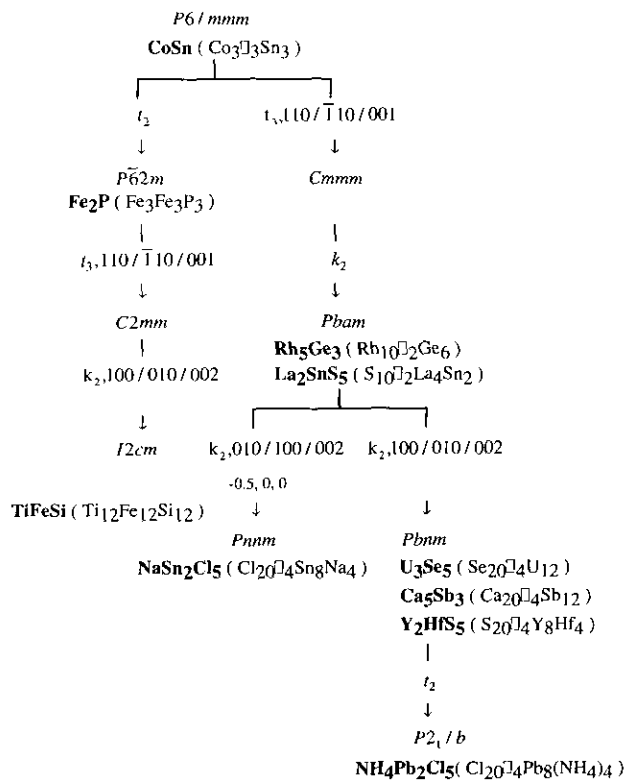

FIG. 6. Space-group relationships of "filled" CoSn-type structures.

$NaSn_2Cl_5$ (distorted Rh_5Ge_3)-type structures then correspond to the TiFeSi (distorted Fe_2P)-type structure (20). In terms of space-group relationships, however, the Fe_2P- and Rh_5Ge_3-type structures, as well as their distorted versions with lower symmetry and doubled pseudohexagonal axes (TiFeSi, U_3Se_5, $NH_4Pb_2Cl_5$, and $NaSn_2Cl_5$), represent different subgroups of *P6/mmm*. This space group is represented by the CoSn-type structure, which may be considered as a higher symmetric defect structure of both the Fe_2P- and the Rh_5Ge_3-type structure with $\frac{1}{2}$ or $\frac{1}{6}$ of the metal positions unoccupied, respectively.

Structure correlations by means of symmetry relations between space groups are to be of practical value. In order to elucidate more clearly the structure relationships between the $NaSn_2Cl_5$-type and the $NH_4Pb_2Cl_5$-type structures, the scheme of their crystal structures is shown in Fig. 7. For La_2SnS_5, two adjacent unit cells are

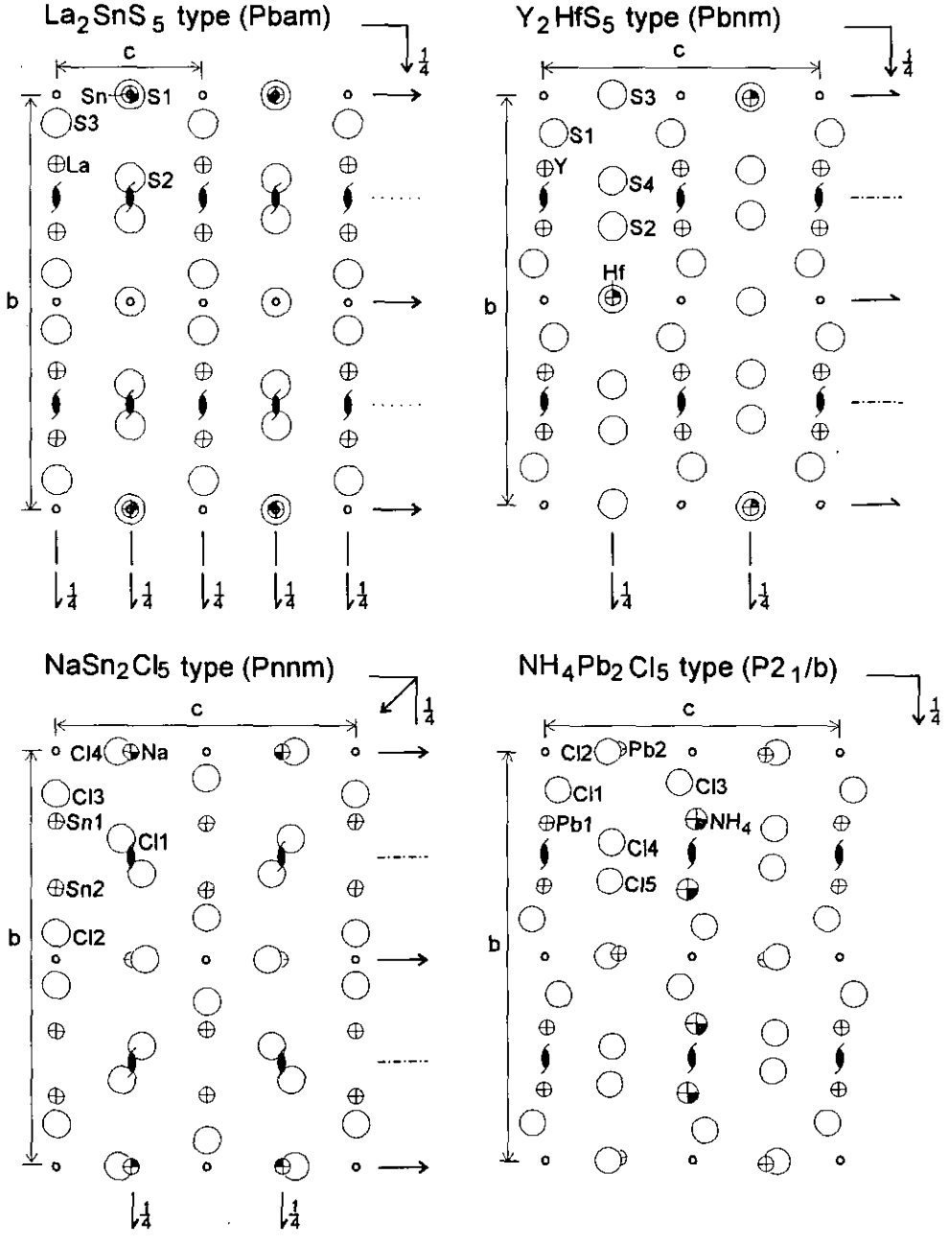

FIG. 7. *Schematic representation of the crystal structures of AB_2X_5 compounds. All symmetry elements of the respective space groups are included in order to show the way of thinning (Auslichtung) during the symmetry reduction.*

included, and for $NaSn_2Cl_5$, the origin is moved to (−0.5, 0, 0). All atoms lie on mirror planes perpendicular to the *c* axis. If one reduces the symmetry by index k_2 leaving out half of the translations in the *c* direction, which is equivalent to doubling the *c* axis, only one-half of the mirror planes, one-half of the inversion centers, and one-half the screw axes can be retained.

ACKNOWLEDGMENTS

We gratefully acknowledge financial support by the Deutsche Forschungsgemeinschaft and the Fonds der Chemischen Industrie.

REFRENCES

1. H. M. Powell and H. S. Tasker, *J. Chem. Soc.*, 119 (1937).
2. P. W. J. Jansen, *Rec. Trav. Chim. Pays-Bas* **87,** 1021 (1968).
3. H.-L. Keller, *Z. Naturfosch. B* **31,** 885 (1976).
4. F. G. Ras, D. J. W. Ijds, and G. C. Verschoor, *Acta Crystallogr. Sect. B* **33,** 259 (1977).
5. H. P. Beck, G. Clicqué, and H. Nau, *Z. Anorg. Allg, Chem.* **536,** 35 (1986).
6. H. P. Beck and H. Nau, *Z. Anorg. Allg, Chem.* **536,** 45 (1986).
7. H. P. Beck and H. Nau, *Z. Anorg. Allg. Chem.* **554,** 43 (1987).
8. G. Rack, *Zentr. Mineral. Geol.*, 378 (1913).
9. H. P. Beck and H. Nau, *Z. Anorg. Allg. Chem.* **558,** 193 (1988).
10. G. Brauer, "Handbuch der Präparatioven Anorganischen Chemie," p. 753. Ferdinand Enke-Verlag, Stuttgart, 1978.
11. LSUCR, Least squares unit cell refinement, Programmbibliothek für die Chemie, HRZ Köln.
12. J. R. Einstein, *J. Appl. Crystallogr.* **7,** 331 (1974).
13. MolEN, An Interactive Structure Solution Procedure, Enraf–Nonius, Delft, The Netherlands, 1990.
14. D. T. Cromer and J. T. Waber, "International Tables for X-ray Crystallography," Vol. IV. Kynoch Press, Birmingham, England, 1974.
15. D. L. Roussean, R. P. Bauman, and S. P. S. Porto, *J. Raman Spectrosc.* **10,** 253 (1981).
16. H. Bärninghausen, *Match* **9,** 139 (1980).
17. S. Geller, *Acta. Crystallogr.* **8,** 15 (1955).
18. W. Jeitschko and P. C. Donohue, *Acta. Crystallogr. Sect. B* **31,** 1890 (1975).
19. K. Schubert, "Kristallstrukturen Zweikomponentiger Phasen," p. 324. Springer-Verlag, Berlin/Göttingen/Heidelberg/New York, 1964.
20. W. Jeitschko, *Acta Crystallogr. Sect. B* **26,** 815 (1970).